INDUSTRIAL AND CIVIL ENGINEERING AND ECONOMICS

DOI 10.15826/rjcst.2019.2.001 УДК 624.042.7

Pierotti A.[1], Leoni M.[2], Lo Presti D.[3]
[1, 3] University of Pisa,
Pisa, Italy
[2] WeSI Geotecnica,
Genoa, Italy
E-mail: [3]diego.lopresti@dic.unipi.it

NUMERICAL ANALYSES OF UNDERGROUND OPENINGS IN COMPETENT ROCK MASSES: CONTINUOUS VS DISCONTINUOUS

Abstract. The paper is aimed at comparing the results of numerical analyses of underground openings in competent rock masses like the Carrara Marble (Italy) by considering a real and well documented case study. More specifically, 3D FEM and DEM analyses were carried out on a rock-mass model interested by two faults and three sets of discontinuities. The geometrical model is representative of deep underground openings where spalling — cracks and rock bursts can occur. PLAXIS 3D and 3DEC were used for the analyses. Intact rock and rock mass characterization of Carrara Marble was inferred from available technical literature. The analysis results were compared in terms of principal stresses and displacements in a number of monitoring points around the opening. The main practical interest is to find out a reliable approach for evaluating the stability of very large openings in a competent rock mass like Carrara Marble. For such a purpose, a number of available in-situ stress measurements were used.

Keywords: FEM analysis, DEM analysis, numerical model, quarry, rock mass strength

Пьеротти А.[1], Леони М.[2], Ло Прести Д.[1]
[1, 3] Университет Пизы,
Пиза, Италия
[2] WeSI Geotecnica,
Генуя, Италия
E-mail: [3]diego.lopresti@dic.unipi.it

ЧИСЛЕННЫЙ АНАЛИЗ ПОДЗЕМНЫХ ОТВЕРСТИЙ В КОМПЕТЕНТНЫХ ГОРНЫХ ПОРОДАХ

Аннотация. Целью данной работы является сравнение результатов численного анализа подземных отверстий в компетентных горных массивах, таких как каррарский мрамор (Италия) на реальном примере с большим количеством данных. Более конкретно анализы 3D FEM и DEM были проведены на модели массива горных пород с двумя разломами и тремя наборами разрывов. Геометрическая модель репрезентативна для глубоких подземных отверстий, где могут возникать сколы — трещины и разрывы горных пород. Для анализа использовались PLAXIS 3D и 3DEC. Характеристики нетронутой породы и скального массива каррарского мрамора были получены из доступной технической литературы. Результаты анализа были сопоставлены с точки зрения основных напряжений и перемещений в ряде контрольных точек вокруг отверстия. Основной практический интерес заключается в том, чтобы найти надежный подход для оценки устойчивости очень больших отверстий в компетентном горном массиве, таком как каррарский мрамор. Для этой цели был использован ряд доступных измерений напряжений на месте.

Ключевые слова: конечно-элементный анализ, метод дискретных элементов, численные модели, карьер, прочность горных пород

Introduction

Underground openings excavated in jointed rock masses at shallow depths may cause structurally controlled instabilities. These instabilities are mainly controlled by the number and orientation of discontinuity — sets or single joints (faults) and by the available

strength along these weakness surfaces. On the other hand, deep underground openings modify the geostatic stress-field causing stress-redistribution and potentially stress-controlled instabilities.

The simplest approach for evaluating the stress field that may be induced by an underground opening is the elastic one [1]. Elastic solutions [2] have the great advantage of simplicity but also several limitations (i.e. oversimplifications concerning the boundary stresses away from the opening, elastic constitutive model and the geometry of the opening(s) among the most relevant). In recent years different types of numerical methods became available. As far as the modeling of the rock mass is concerned, the following approaches are available: a) to consider the rock mass as a continuous medium with reduced strength and stiffness characteristics with respect to the intact rock (i.e. a sort of homogenization process depending on the number and types of discontinuities, namely equivalent continuum), b) to consider the rock mass as a discontinuum consisting of intact rock and very few discontinuities or c) to use hybrid continuum/discontinuum approaches. The continuum methods include Finite Difference Method (FDM), Finite Volume Method (FVM), Finite Element Method (FEM) [3, 4], Meshless Method, Boundary Element Method (BEM). Discontinuum methods include Discrete Element Method (DEM) [5, 6], Discrete Fracture Network Method (DFN). Various researchers [see as an example 7, 8] provided an overview of such methods also considering the hybrid ones.

Usually the choice of analysis approach depends on the scale of the problem. According to Barton [9], in case of tunnelling, discontinuum model is considered appropriate for a range of Q ≈ 0.1–100 (Fig. 1). As far as the continuum approach is concerned, the Finite Element Method (FEM) enables one to deal with heterogeneous rock masses. Moreover, constitutive models, incorporating elasto-plasticity and viscosity, can be adopted in FEM analyses. Failure analysis, cracking as well as finite displacement along discontinuities or rotations cannot be treated by conventional FEM approach because of the continuum assumption. Continuous re-meshing or hybrid approach can overcome such a limitation. On the other hand, the effectiveness of discontinuum approach mainly depends on the availability of sufficient geological and geomechanical data.

Nowdays the continuum approach is still the most popular and few Authors have tried to compare the results of these two types of analyses in real cases [8–11]. On the other hand, in the case of layered structures (i.e. shale formations), where the rock mass behaviour is mainly controlled by the set of discontinuities, it could be convenient to use the continuum approach. Therefore, parametric studies have shown in which way the anisotropic behaviour of these types of rock masses can be well simulated by using the continuum approach (see as an example, [12] or [13]). The case study does not belong to this category because it concerns a competent rock mass with few discontinuity sets. This paper deals with a real and well documented case study. According to Scavia [14] we believe that equivalent continuum and discontinuum approaches may lead to very different results. Therefore, these approaches should be used for different purposes and objectives. Our aim is to compare, in terms of principal stresses and displacement vectors, the results of 3D continuous and discontinuous analyses that were carried out by using PLAXIS 3D [15] and 3DEC [16]. The study model consisted of an "idealized" rock mass block (700×400×595 m) interested by two faults and three sets of discontinuities. These structural features correspond to those observed around an existing deep quarry, as better explained later on. The opening is 49×50×30 m and the floor is 95 m above the block-bottom (Fig. 2). The geomechanical characterization of the rock mass, intact rock and discontinuities was inferred from the technical literature.

Carrara marble is extracted from the mining district of Carrara in the North-West Tuscany (Italy). It is a ge-

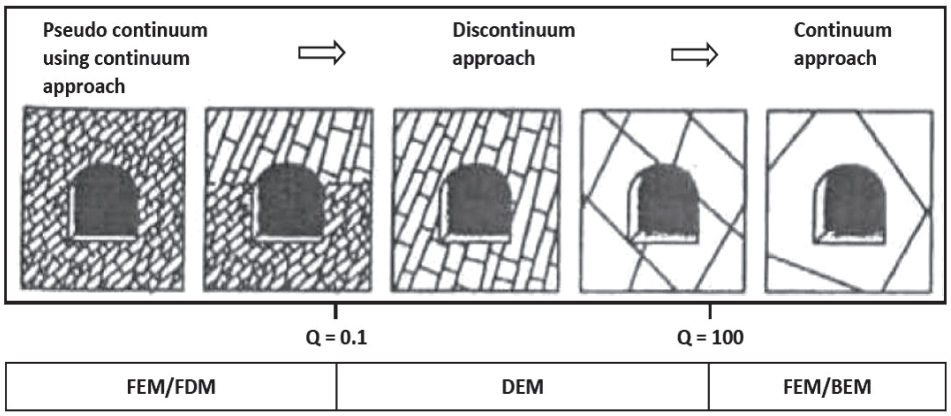

Fig. 1. Schematic diagram suggesting the range of application of discontinuum modeling in relation to *Q* value ([9] modified by [10]). For the study case *Q* is about 7; RMR = 9 · LNQ+44

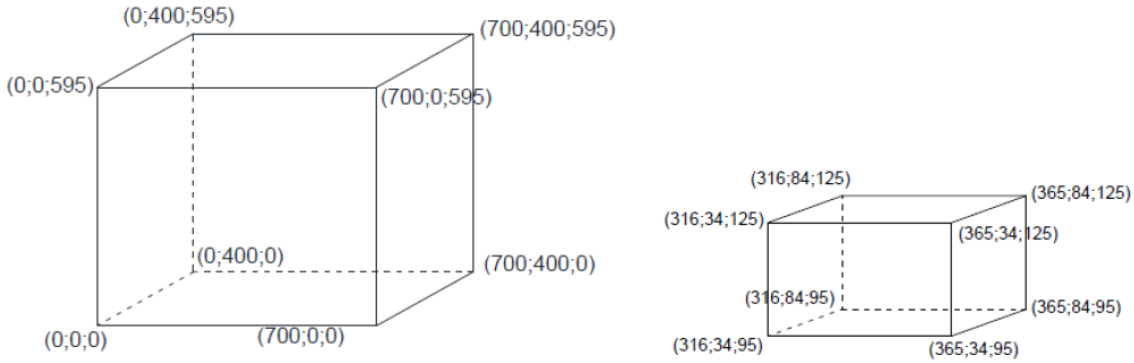

Fig. 2. Absolute coordinates (x, y, z) of the block (on the left) and of the internal cavity (on the right)

neric term indicating different commercial products of a carbonate metamorphic rock. More specifically the so-called "Bianco di Carrara" is considered in the present study. The mining district is actually very wide and the mine exploitation is carried out in different ways.

The paper firstly summarizes the mechanical characterization and classification indexes of Carrara marble from the available technical literature. This was done for exploring the variability of the interest parameters (strength and stiffness of both intact rock, rock mass and discontinuities) within the whole mining district. In a second step, specific model parameters for FEM and DEM analyses were selected from the published data. In other words, the Authors intend to perform independent FEM and DEM analyses by using the specific available parameters.

1. Materials and methods

1.1. Geomechanical characterisation of the Carrara marble

The geomechanical characterization of Bianco di Carrara is based on a number of research papers [17–20]. Table 1 and 2 summarize the geomechanical characterization and the classification indexes of "Bianco di Carrara" as inferred from literature [17–20]. The strength and stiffness parameters specifically used for the numerical analyses are summarized later on. In these tables, values referred to x, y, z directions were obtained from laboratory testing on groups of specimens drawn from three perpendicular directions, of which z is directed orthogonal to the apparent marble layering [20]. Shear strength of intact rock (τ) was evaluated by means of di-

Table 1

Mechanical characterization of Carrara marble from literature

Quarry	Symbol	Ravaccione Fantiscritti	Carrara	Carrara		
				x	y	z
Overburden on average	[m]	440	760			
	γ [N/m^3]	26500		27170	27170	27170
	$k_1 = \sigma_2/\sigma_1$	0.59				
	$k_2 = \sigma_3/\sigma_1$	0.33				
Uniaxial Compressive Strength (intact rock)	σ_c [MPa]	99.65	84.70	101.4	96.6	101
Tensile Strength (Direct Tensile Strength or Hydraulic Fracturing)	σ_t [MPa]		25.8 (HF)	8.4	9.9	6.9
Tensile Strength (Brasilian test)	σ_t [MPa]		6.11	11.5	9.8	9.9
Tangent Young Modulus compression	E_t [GPa]	61.14	52.80	67	62.1	59.4
Tangent Young Modulus in tension	E_t [GPa]			59.5	60.6	39.9
Secant Young Modulus	E_s [GPa]	39.037				
Tangential Poisson's ratio	ν_t	0.25	0.23	0.28	0.28	0.27
Secant Poisson's ratio	ν_s	0.136				
Dynamic Young modulus	E_{dyn} [GPa]		68.50	66	64.9	62.4
Dynamic Poisson ratio	ν_{dyn}			0.34	0.34	0.31
Cohesion	c [MPa]	28	24.60	16.7	25.7	23.1
Friction angle	Φ [°]	32	33.60	42.4	33.3	37.8
Shear Strength of Intact Rock (for σ_n = 3.5 MPa)	τ [MPa]			18.2	18.5	15.2

Table 2

Classification indexes of Carrara marble from literature

Quarry	Symbol	Ravaccione Fantiscritti	Carrara	Carrara		
				x	*y*	*z*
RMR	RMR	61				
RMR (absence of water)		66				
GSI		56				
GSI (absence of water)	GSI	61				
HOEK–BROWN STRENGTH CRITERION						
	GSI	61	63–67			
	σ_{ci} [MPa]	99				
	m_i	9	5.94	12.5	6.95	8.09
	D	0				
	s	0.01	0.02	1	1	1
	a	0.50				
	m_b	2.24	1.70			

Table 3

Geometrical and mechanical characteristics of major discontinuities in Ravaccione and Fantiscritti open pit (Carrara)

	System	Dip [°]	Dip Direction [°]	JRC	JCS	JKN [MPa]	JKS [MPa]	Φ_b [°]	Φ [°]	c [MPa]
Ravaccione (Carrara)	K1	88	359	4–6	96.5	40000	19000	32.3	45	11.2
	K2	54	105	3–5	88.4					
	K3	80	54	2–4	41.5					

rect shear tests on intact specimens that were subjected to a normal stress σ_a = 3.5 MPa.

Tables 3 to 5 show the geomechanical characterizations of discontinuities as inferred from existing technical literature.

Table 3 shows the characteristics of discontinuities surveyed in the Ravaccione & Fantiscritti pit [18]. The mechanical characterization of these discontinuities was obtained by laboratory tests, carried out according to ISRM suggested methods [18]. Table 4 concerns discontinuities surveyed in another quarry [19]. Table 5 refers to artificial discontinuities that have been prepared and tested in the lab [20]. It is worth mentioning that in Table 3 the reported value of cohesion was inferred from a specific analysis trying to account for the existence of rock bridges. The cohesion value of Table 5 was instead experimentally determined in the lab on artificial discontinuities.

Table 4

Mechanical characteristics of discontinuity (open pit near Pianza anticlinal — Carrara)

	Φ_p [°]	c_p [MPa]	Φ_r [°]	c_r [MPa]	Φ_b [°]
Pianza (Carrara)	34	0.71	34	0.51	32

Table 5

Characterization of artificial discontinuities of Carrara marble samples

	Φ_p [°]	c_p [MPa]	Φ_r [°]	c_r [MPa]
Carrara	36	0.7	36	0.5

It is worth nothing that, while the intact rock and rock mass exhibit rather homogeneous parameters, as for the discontinuities certain variability is observed. Moreover, as for the m_i parameter (HB criterion [21, 22]), the values are mainly within the range 6–9. A small scatter is instead observed for the *s* parameter (0.01–0.02). These values are consistent with the average GSI.

1.2. Numerical methods

This paper aims to compare FEM and DEM methods in order to outline limitations and capabilities of these different approaches, in the specific field of underground excavations. The comparison concerns a 3D model of a blocky rock mass containing a cavity. The case study represents an idealization/simplification of the Ravaccione Fantiscritti Quarry. Indeed the sets of discontinuities correspond to those effectively observed [18], while the geomechanical characterization was inferred from those reported in Tables 1 to 5.

As for the numerical analyses the adopted geomechanical characteristics are reported in Tables 6 to 9. The geometry and geomechanical characterization of the two joints were arbitrarily established. FEM and DEM analyses were carried out using respectively Plaxis 3D [15] and 3DEC [16]. 3DEC is a specific tool, based on the distinct element method. This program allows one to model a jointed rock mass as a series of discrete and deformable blocks. Dimensions and geometry of the blocks depend on fracturing characteristics of rock: orientation and spacing of natural discontinuity contained in

the rock mass are fundamental. Discontinuities between blocks are considered as boundary conditions for each block. These conditions are determined by the characterization of the discontinuities that are considered as zones of interaction between blocks. For each discontinuity an appropriate behavior model must be assumed. This type of modeling allows large displacements along the discontinuities as well as the rotation of the blocks, by means of an explicit algorithm. As for the constitutive model, it is possible to consider time-dependent and both linear and non-linear constitutive relations for the rock matrix and for the discontinuities. The DEM code also allows assimilating the behavior of each block to that of a rigid body or a deformable body. For some applications the deformation of the individual blocks can be ignored while, if not, it can be accounted by the discretization of each block to the finite differences. In the latter case, each block is further subdivided with a finite difference meshing. The Mohr–Coulomb (MC) criterion was adopted both for the rock mass and for the discontinuities.

$$\tau = c' + \sigma'_n \tan\Phi \qquad (1)$$

where τ and σ'_n are the tangential and normal stresses on the failure plane at failure, respectively, c is the cohesion of the intact rock and Φ is the angle of shear resistance.

Table 6

Stiffness and strength parameters for DEM model

γ [kN/m^3]	C [MPa]	Φ [°]	K [GPa]	G [GPa]	σ_t [MPa]
27	20	37	29.5	25	8

(K = bulk modulus, G = shear modulus).

Mechanical parameters (Table 6) adopted for the rock matrix were inferred from those reported on Table 1. Plaxis 3D is a finite element program used in geotechnical field. An equivalent continuous model was defined in order to use such a numerical analysis. Indeed, in the case of continuous equivalent models we renounce to the thorough modeling of all the discontinuities whilst the parameters of the intact rock are appropriately reduced to take into account the rock mass weakening because of the existence of various set of discontinuities. The Hoek–Brown (HB) criterion [21, 22] was adopted for the rock mass. The Hoek–Brown failure criterion expresses the resistance of the rock through a non-linear relationship between the principal stresses:

$$\sigma'_1 = \sigma'_3 + \sigma_c \left(m_b \frac{\sigma'_3}{\sigma_c} + s \right)^a \qquad (2)$$

where σ'_1 and σ'_3 are the major and minor principal stresses, m_b and s are dimensionless empirical constants of the rock mass and σ_c is the uniaxial compressive strength of the intact rock. This criterion assumes that the failure behavior of a rock mass can be assimilated to that of an equivalent continuous medium. The constants m_b and s can be properly scaled according to the type of rock under examination and to the geological-structural arrangement of the rock mass, using these expressions:

$$m_b = m_i \cdot \exp\left(\frac{\mathrm{GSI} - 100}{28 - 14D} \right), \qquad (3a)$$

$$s = \exp\left(\frac{\mathrm{GSI} - 100}{9 - 3D} \right), \qquad (3b)$$

$$a = 0.5 + \frac{1}{6} \cdot \left(e^{-GSI/15} - e^{-20/3} \right). \qquad (3c)$$

According to the Bienawski rating system [23], the rock mass is characterized by a GSI = 66. The Hoek–Brown parameters have been so calculated considering GSI = 66, D = 0, σ_c = 99 MPa and m_i equal to 9 (intact rock), as indicated by some authors for Carrara marble [18].

Table 7

Stiffness and strength parameters for FEM model

γ [KN/m^3]	E [KN/m^3]	ν [–]	σ_c [MPa]	σ_t [MPa]
27	$5.85 \cdot 10^7$	0.17	100	8

For modulus G, K, E and the Poisson's ratio ν reported in Table 6 and in Table 7 the following relations apply

$$G = E / (1 + 2\nu), \qquad (4)$$

$$K = E / 2 \cdot (1 - 2\nu). \qquad (5)$$

It is worth mentioning that, the set of parameters for DEM and FEM analyses were indepentely inferred fron available literature data. Consequently a different σ_c was considered. In particular the uniaxial compression strength was considered equal to 80 MPa for the DEM analyses while was equal to 99 MPa in FEM analyses. In other words we would approach the analyses such as a practizing engineer using different computational tools that require different sets of input parameters. Anyway, the adopted MC (intact rock) and HB (GSI = 100) criteria can be considered equivalent as better shown later on.

1.3. Model geometry and monitoring points

The model used for numerical analysis represents a rock mass block (700×400×595 m) containing an opening/cavity (49×50×30 m). The opening's sides are parallel to the block's one. Fig. 2 shows coordinates (x, y, z) respectively of the whole block (at the left) and of the opening (at the right). The block is crossed by two faults and by three sets of discontinuities (K1, K2, K3). Table 8 shows orientation and mechanical characteristics of the faults. The orientation is defined by two angles: the dip-direction angle (dd), measured in the global xy-plane, clockwise from the positive y-axis and the dip angle (dip) measured in the negative z-direction from the global xy-plane.

Table 8

Geometrical and mechanical characteristics of the two faults

	dip [°]	dd [°]	JKN [MPa/m]	JKS [MPa/m]	Φ [°]	c [MPa]
Fault 1	66	253	30	10	20	0.01
Fault 2	63.03	100	3000	1000	30	5

JKN and JKS are the joint normal stiffness and joint shear stiffness. The same table shows Mohr–Coulomb parameters, cohesion and friction angle, adopted for the characterization of discontinuities. Table 9 shows orientation and mechanical characteristics of the three sets of discontinuities. JRC and JCS are respectively the joint roughness coefficient and the joint wall compressive strength. In order to compare the results of the analysis, an array of 40 monitoring points has been chosen. Points are located around the openings or directly on their sides, along three vertical sections parallel to the *xz* plane, i. e. the vertical plane ($y = 36$, $y = 59$, $y = 82$) (Fig. 3).

2. Results

The outputs of the numerical analyses were compared in terms of principal stresses and displacements. Fig. 4 shows the major and minor principal stresses as obtained from FEM and DEM analyses for 20 monitoring points. The figure also shows the considered strength envelopes (Mohr & Coulomb and Hoek & Brown).

The linear Mohr–Coulomb envelope was cut at $\sigma_3 = -8$ MPa, that is the tensile strength of Carrara marble (Table 1). As for the HB criterion, both the case for GSI = 100 (intact rock) and that for GSI = 66 are shown in Fig. 4.

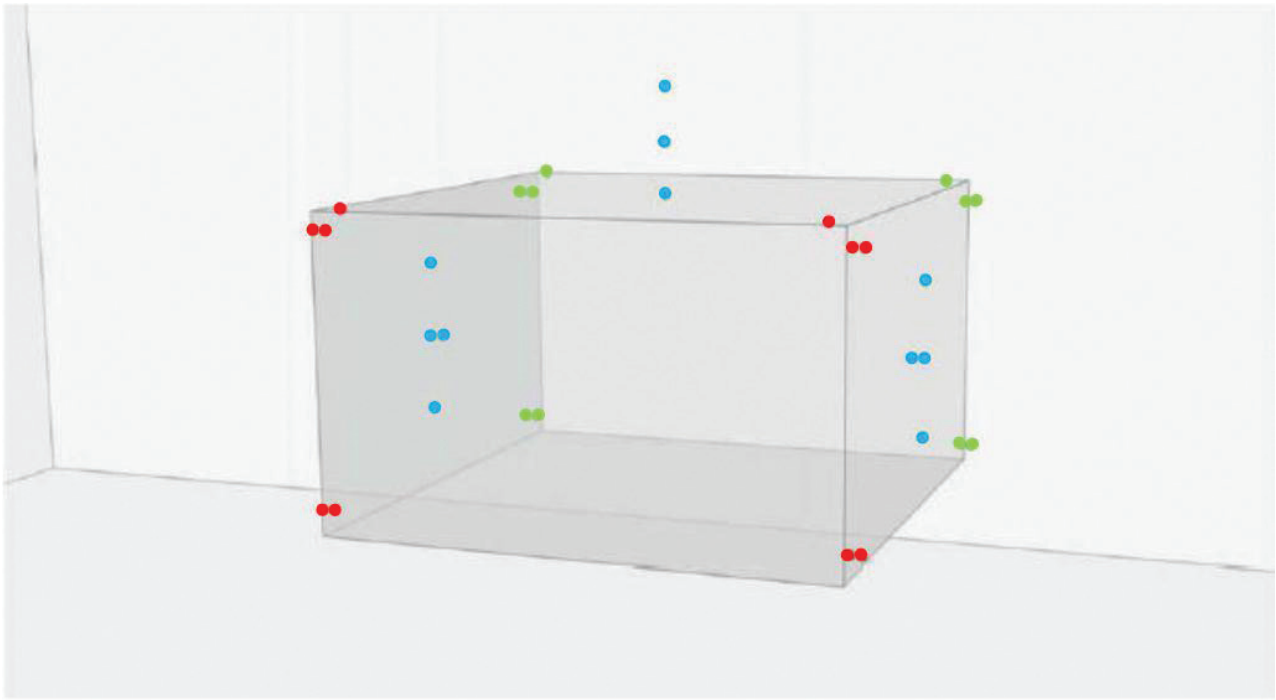

Fig. 3. Location of the monitoring points around the cavity

Table 9

Geometrical and mechanical characteristics of discontinuity sets

	No of discontinuities	dip [°]	dd [°]	JRC	JCS	JKN [MPa/m]	JKS [MPa/m]	F [°]	c [MPa]
K1 (2m)	5	88	359	4–6	96.5	40	19	32.3	11.2
K2 (4m)	5	54	105	3–5	88.4	40	19	32.3	11.2
K3 (4m)	5	80	54	2–4	41.5	40	19	32.3	11.2

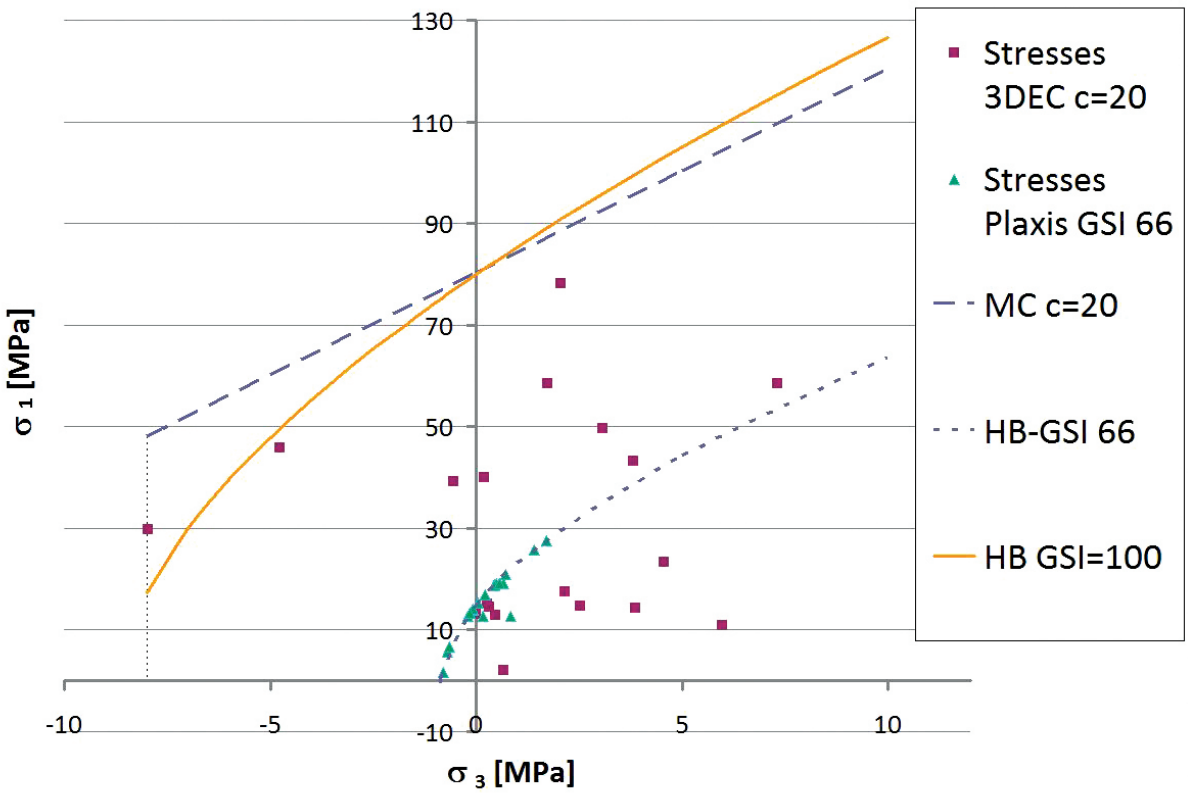

Fig. 4. Failure envelopes (MC & HB) in the principal stresses plane and stresses values inferred from PLAXIS & 3DEC analyses

The MC criterion (intact rock) and that by HB (GSI = 100) mainly coincide for the relevant stress interval. In the following, stresses and cohesion are in MPa even if not explicitly indicated.

PLAXIS provides values of σ_1 and σ_3 mostly lower than those obtained from 3DEC analyses (Fig. 4). In particular the principal stresses, as inferred from PLAXIS analyses, are very close to the adopted curvilinear failure envelope or lay on it. On the other hand, in the discontinuous model, the induced stresses are always well below the linear failure envelope i.e. MC (intact rock) (Fig. 4).

Figs. 5, 6 and 7 directly compare similar stress components (σ_1, σ_3, τ_{max}) as obtained from PLAXIS and 3DEC analyses at the various monitoring points. These Figures confirm what observed in Fig. 4.

Table 10 shows the maximum displacements obtained by PLAXIS in the three directions *x*, *y*, *z*. Table 11 shows the values of the maximum principal stresses obtained by the two programs on the whole model with the relative point's coordinates. Graphic outputs of 3DEC show a max displacement of about 40 cm, in the section parallel to the *xz*-plane and passing through the center of the chamber, at the intersection between the chamber itself and the K3 discontinuity set. Still in the vicinity of the room, but outside the intersection with the K3 set, displacements vary between 1 and 2 cm and are therefore comparable with those obtained from PLAXIS.

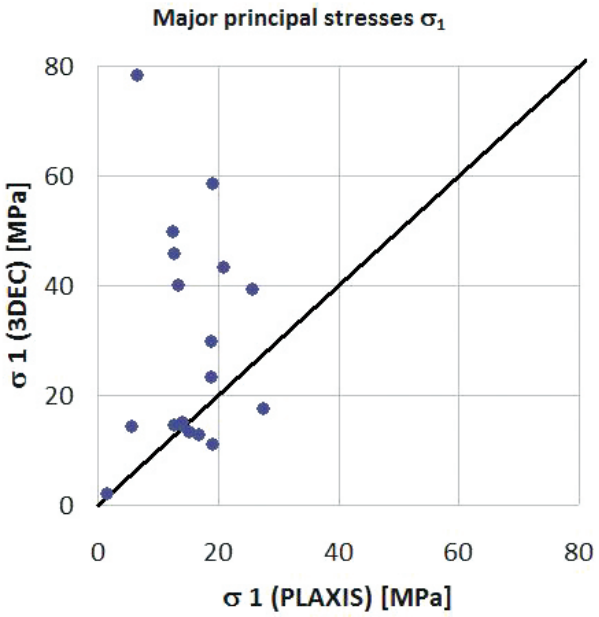

Fig. 5. Major principal stresses at the monitoring points

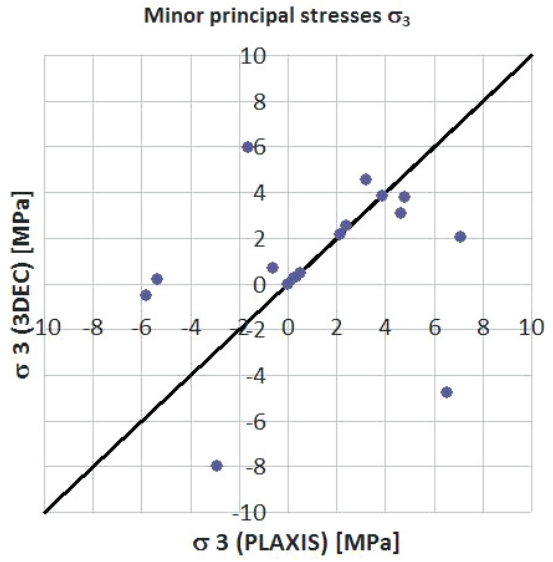

Fig. 6. Minor principal stresses at the monitoring points

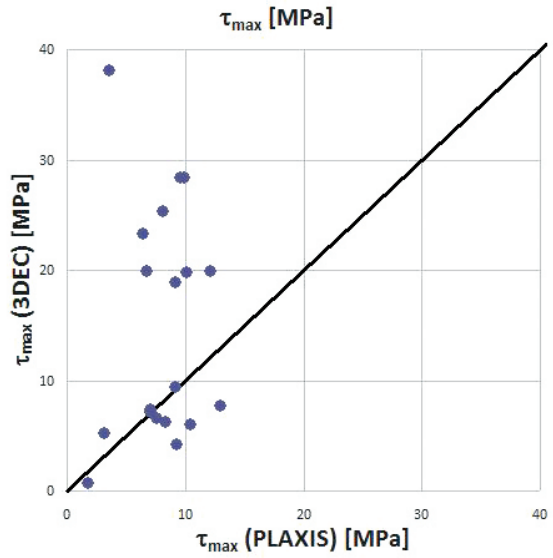

Fig. 7. Maximum shear stresses at the monitoring points

Table 10

Maximum displacements obtained from PLAXIS for the three directions *x*, *y*, *z*

	$\|u_{max}\|$ [mm]	*x* [m]	*y* [m]	*z* [m]
u_x	13.5	365.0	66.4	103.6
u_y	5.2	336.2	34.0	103.0
u_z	12.9	333.02	66.1	95.0

Fig. 4 clearly shows that the adopted strength envelopes for FEM and DEM analyses cannot lead to comparable results. Therefore, a new set of Mohr–Coulomb parameters (*c*' and Φ') was evaluated by best fitting the Hoek–Brown envelope (for the given σ_c, GSI, m_i and *D*). Interpolation was carried out within a specific interval of the minor principal stress (σ_3) by using RocLab [24]. On the other hand, considering the first set of Mohr–Coulomb parameters (*c* = 20 MPa and Φ = 37°) that have been used for the DEM analyses, a new set of HB parameters was estimated in order to have a Hoek–Brown criterion equivalent to the MC (intact rock) one.

In this case the value of σ_c was kept equal to 99 MPa. The old and the new set of parameters are shown in Table 12. Numerical analyses were repeated by considering the new sets of parameters and the results are shown in Fig. 8 that also shows the four strength envelopes.

Table 12

Hoek–Brown and Mohr–Coulomb criterion, equivalent parameters for σ_{3max} = 24.75MPa

Hoek–Brown (PLAXIS)		Mohr–Coulomb Fit Parameters		Mohr–Coulomb (3DEC)		Hoek–Brown Fit Parameters	
σ_c	99 Mpa	*c*	6.34 MPa	*c*	20 MPa	σ_c	99 MPa
GSI	66					GSI	98
m_i	9	Φ	34.2°	Φ	37°	m_i	6
D	0					*D*	0

It is possible to see that DEM, in any case, gives higher stresses than that predicted by FEM analyses. Anyway, the differences appear less dramatic especially when comparing the FEM results with GSI = 66 to those from DEM analyses with c = 6.3 MPa and Φ = 34.2°.

3. Discussion and closing remarks

The UOIM of the USL1 of Massa Carrara (i.e. the public body responsible for the safety during mining activities in the Carrara District) [18] performed a number of in situ stress measurements. Measurements mainly concerned the Ravaccione and Fantiscritti quarries. More specifically the in situ stresses were estimated by different techniques, namely: Hydraulic Fracturing, Doorstopper and Triaxial Thin Hollow Inclusion (CSIRO type cell). This last technique provided most reliable data. According to [18], the obtained results demonstrated that the stress state originated in the study area differs from the lithostatic one.

Table 11

Maximum and minimum principal stresses from PLAXIS and 3DEC.

	σ [MPa] PLAXIS	*x* [m]	*y* [m]	*z* [m]	σ [MPa] 3DEC	*x* [m]	*y* [m]	*z* [m]
σ_{1max}	70.19 (compression)	346.07	0.00	0.00	116 MPa (compression)	365	59	96
σ_{1min}	–1.464 (traction)	320.30	61.30	95.00	–2 MPa (traction)	350	59	88
σ_{3max}	11.57 (compression)	346.07	0.00	0.00	9.36 MPa (compression)	365	59	96
σ_{3min}	–7.77 (traction)	360.41	39.08	95.00	–8 MPa (traction)	320	59	125

Moreover, they found the both FEM and DEM back — analyses gave a consistent estimate of in situ stresses.

The UOIM also endorsed an experimental approach for the safety evaluation of the quarries within the Carrara Mining District [25]. The approach consists of an accurate assessment of: geometry & morphology, geostructural characteristics, in situ stress measurements, geomechanical characterization in the lab, monitoring of stress and displacements, calibration of numerical models (continuous and discontinuous). Their conclusions agree with [18]. Moreover they pointed out the following facts:

- needs for continuous monitoring of stress-strain during excavation by the use of appropriate stressmeters;
- needs for using DEM models.

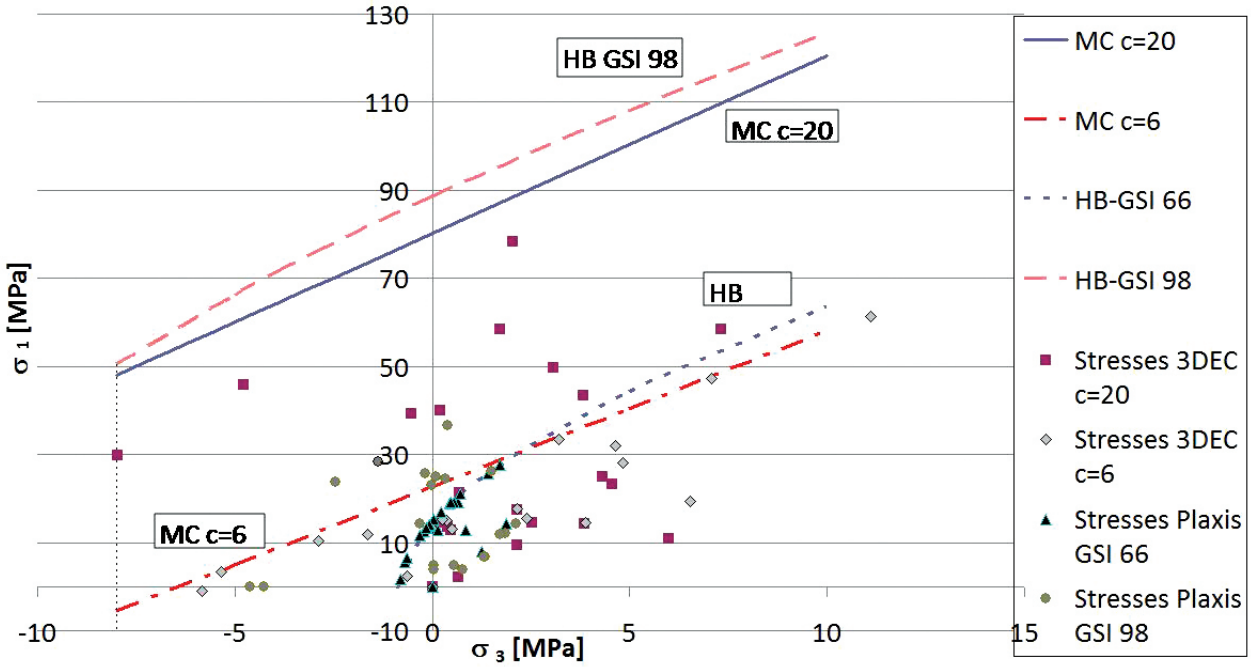

Fig. 8. Equivalent failure envelopes (MC & HB) in the principal stress plane and stress values from PLAXIS & 3DEC at the monitoring points

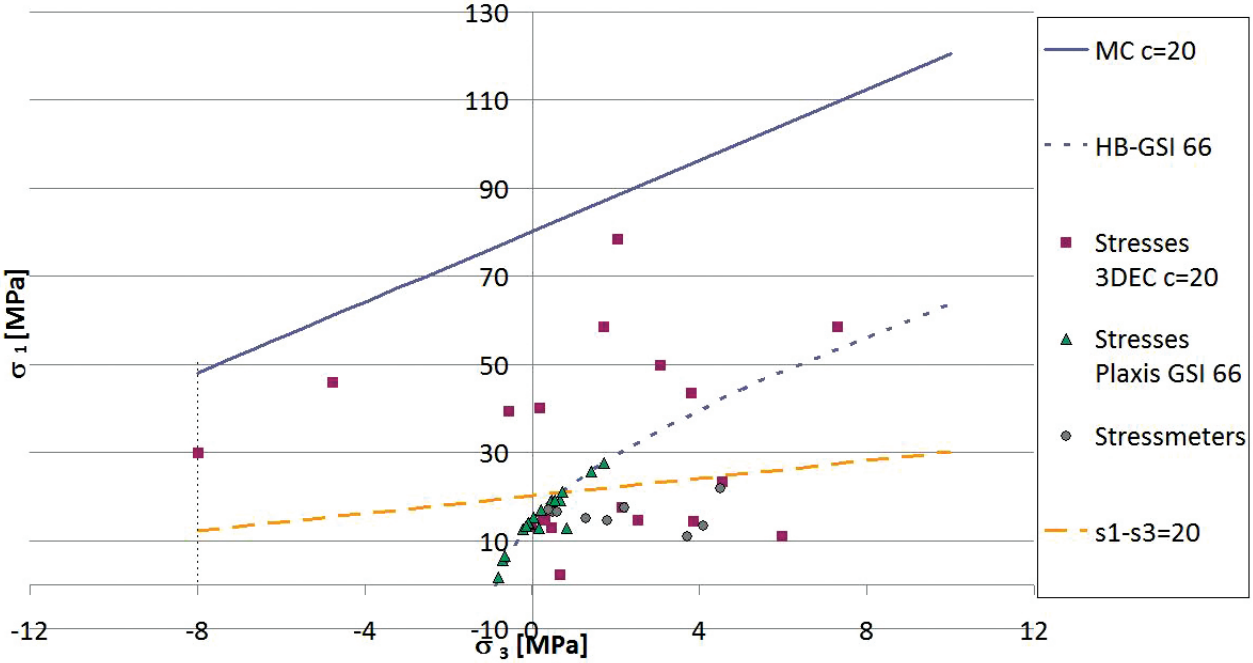

Fig. 9. Failure envelopes (Tresca type, MC and HB), in situ principal stress measurements and those inferred from 3DEC and PLAXIS analyses

More importantly they provided an empirical conservative, specific strength criterion. In particular, they enveloped the stress conditions of those locations where crack initiation had been observed. The envelope was established according to a Tresca-type criterion ($\sigma_1 - \sigma_3 = 20$ MPa $\approx 0.2\sigma_c$) [25] which is equivalent to an undrained Mohr–Coulomb criterion ($C_u = 10$ MPa, $\phi' = 0$). Eventually, we performed an analysis by considering the above strength criterion. The results are summarized in Fig. 9. The same figure also shows the stress state measurements (safe condition) carried out by [25].

In conclusion the paper confirms the ability of DEM-based analyses to predict large displacements, in any case much larger than those obtained by using FEM analyses. This result should be considered as preliminary and confirmed through additional comparisons by increasing the number of monitoring points. More importantly, it is worthwhile to point out that the results of FEM analysis, in terms of stresses, appear much more realistic if compared with the stress-field monitoring. With this respect, the use of FEM analysis appears more appropriate even in the case of a very competent rock mass, which is really a surprising result. For the considered case, the differences between DEM and FEM analysis could be explained by considering the adopted failure criterion and strength parameters. Indeed, the obtained results suggest that the MC strength parameters of intact rock and discontinuities and the HB strength parameters of rock mass (as inferred from literature data) lead to a completely different pattern of stress distribution around the opening. In particular, when the MC strength parameters are re-calibrated in order to fit the HB strength criterion, the differences in terms of stresses become less dramatic (in any case, the MC and HB criteria are not comparable as for the tensile stress field because of their intrinsic nature).

As a final comment of practical interest, the nature of the Carrara marble (few sets of discontinuities, low persistence of discontinuities and existence of strong rock bridges) suggests the possibility of excavating very large cavities. In practice, this could be not safe and the adoption of a conservative strength criterion, as well as of continuous monitoring are strongly recommended.

References

1. Kirsch G. Die theorie der elastizitat und die bedurfinisse der festigkeitslehre [The theory of elasticity and the requirements of strength theory]. *Zentralblatt Verein Deutscher Ingenieure*, 1898, vol. 42, no. 28, pp. 797–807.

2. Hoek E., Brown E. T. *Underground excavations in Rock*. CRC Press, 1982, 532 p.

3. Clough R. W. The finite element method in plane stress analysis. *Proceedings of Second ASCE Conference Electronic Computations*. Pittsburg, 1960. 35 p.

4. Zienkiewicz O. C. *The finite element method in engineering sciences*. 3rd ed. New York, McGraw-Hill, 1977. 521 p.

5. Cundall P. A. A computer model for simulating progressive, large scale movements in blocky rock systems. *Proceedings of the International symposium Rock Fracture (ISRM)*, 1971, vol. 2, paper no. II-8.

6. Cundall P. A. *Technical report MRD-2–74. Rational design of tunnel supports: a computer model for rock mass behaviour using interactive graphic for the input and output of geomaterial data*. Omaha, 1974. 195 p.

7. Nikolic M., Roje-Bonacci T., Ibrahimbegovic A. Overview of the numerical methods for the modelling of rock mechanics problems. *Tehnicki vjesnik*, 2016, vol. 23 (2), pp. 627–637.

8. Scheldt T. Comparison of Continuous and Discontinuous Modelling for Computational Rock Mechanics. *Proc. of 10th ISRM Congress*. Sandton, 2003, 6 p.

9. Barton N. Quantitative description of rock masses for design of NMT reinforcement. *Proc. of Int. Conf. on Hydro Power Development In Himalayas*. Shimla, 1998, pp. 379–400.

10. Barla G., Barla M. Continuum and discontinuum modelling in tunnel engineering. *Rudarsko-geolosko-naftni zbornik*, 2000, vol. 12, pp. 15–35.

11. Barla G., Barla M., Repetto L. Continuum and discontinuum modelling for design analysis of tunnels, *Proc. of 9th Int. Congr. On Rock Mech*. Paris, 1999, 6 p.

12. Sainsbury B. L., Sainsbury D. P. Practical Use of the Ubiquitous-Joint Constitutive Model for the Simulation of Anisotropic Rock Masses. *Rock Mechanics and Rock Engineering*, 2017, vol. 50, pp. 1507–1528.

13. Riahi A., Curran J. H. Full 3D finite element Cosserat formulation with application in layered structures. *Applied Mathematical Modelling*, 2009, vol. 33, pp. 3450–3454.

14. Scavia C. Continuous and discontinuous approaches in rock mechanics and rock engineering. *Rivista Italiana di Geotecnica, XV Croce Lecture*, 2019, vol. 53 (2), 8 p.

15. Brinkgreve R. B. J., Kumarswamy S., Swolfs W. M. *Plaxis 3D Manuals.* Delft, Plaxis, 2017. 470 p.

16. ITASCA Consulting group, Inc. (1993). *UDEC/3DEC*. Available at: http://www.itascacg.com/software/udec.

17. Ferrero A., Migliazza M., Segalini A. In situ fracturing mechanics stress measurements to improve underground quarry stability analyses. *Proceedings of the 3rd CANUS Rock Mechanics Symposium*. Toronto, 2009, pp.1–8. Paper 3964.

18. Ferrero A., Migliazza M., Segalini A., Gulli, D. In situ stress measurements interpretations in large underground marble quarry by 3D modeling. *International Journal of Rock Mechanics & Mining Sciences*, 2013, vol. 60, pp. 103–113.

19. Cravero M., Gulli D., Iabichino G., Nacci F., Valentino D. Geomechanical characterization and numerical modelling of an open pit and underground marble quarry. *Proc. of ISRM Int. Symp. — EUROCK 2002.* Madeira, 2002, pp. 571–578.

20. Cravero M., Gulli D., Iabichino G. Comparative mechanical characterization of marble by means of laboratory testing. *Proc. of 12th Panamerican Conf. on soil Mech. And Geothec. Eng. Soil Rock, 39th U. S. Rock Mech. Symp*. Cambridge, 2003.

21. Hoek E., Brown E. Practical estimates of rock mass strength. *Int. J. Rock Mech. Min. Sci.*, 1997, vol. 34 (8), pp. 1165–1186.

22. Hoek E., Carranza-Torres C., Corkum B. Hoek-Brown failure criterion — 2002 Edition. *Proc. NARMS-TAC Conference*. Toronto, 2002, vol. 1, pp. 267–273.

23. Bieniawski Z. *Engineering rock mass classification*. New York, Wiley, 1989. 272 p.

24. ROCLAB, ROCSCIENCE. V.1.031. *Rock mass strength analysis, software freeware*. Toronto, 2007.

25. Gulli D., Pellegri M. Stress analysis on Carrara marble quarries. *Proc. of 6th Int. Symp. on In-Situ Rock Stress*. Sendai, 2013, pp. 1–18.